Received: 30 January 2023 | Revised: 2 May 2023 | Accepted: 3 May 2023

DOI: 10.1002/chir.23580

RESEARCH ARTICLE

Chirality WILEY

Comparison of different density functional theory methods for the calculation of vibrational circular dichroism spectra

Jonathan Groß | Jonas Kühlborn | Stefan Pusch | Carina Weber | Lars Andernach | Galit Renzer | Paul Eckhardt | Jan Brauer | Till Opatz

Department of Chemistry, Johannes Gutenberg University, Mainz, Germany

Correspondence
Till Opatz, Department of Chemistry, Johannes Gutenberg University, Duesbergweg 10–14, 55128 Mainz, Germany.
Email: opatz@uni-mainz.de

Funding information
Alliance for High Performance Computing in Rhineland-Palatinate; Gauss Alliance e.V.

Abstract

The determination of the absolute configuration (AC) of an organic molecule is still a challenging task for which the combination of spectroscopic with quantum-mechanical methods has become a promising approach. In this study, we investigated the accuracy of DFT methods (480 overall combinations of 15 functionals, 16 basis sets, and 2 solvation models) to calculate the VCD spectra of six chiral organic molecules in order to benchmark their capability to facilitate the determination of the AC.

KEYWORDS

absolute configuration determination, basis set, benchmark, DFT, functional, solvation, VCD

1 | INTRODUCTION

In 1874, van't Hoff included the spatial configuration of aliphatic carbon atoms into organic structural formulae.[1] The first experiments to determine the absolute configuration (AC) of an organic molecule were reported by Bijvoet et al. not earlier than 1951. These authors used X-rays, more precisely zirconium K_α radiation, to assign the configuration of sodium rubidium tartrate using anomalous dispersion. Thereby, they confirmed Fischer's convention, who had previously ascribed the correct AC to L-(+)-tartaric acid.[2]

The correct determination of the AC of organic molecules is crucial to many areas such as asymmetric catalysis, natural product total synthesis, or pharmaceutical applications. Circular dichroism (CD) is one of the chirality-sensitive optical properties of molecules and can be exploited in combination with quantum-mechanical calculations for the assignment of the AC while no chemical derivatization or reference system is needed.[3,4] This phenomenon is based on the differential absorption of left- and right-circularly polarized light by a given molecule, resulting in mirror image CD spectra of a pair of enantiomers.[5] The visible–ultraviolet spectral region is used for electronic CD (ECD) as higher energy photons cause electronic excitations (e.g., $n \rightarrow \pi^*$ or $\pi \rightarrow \pi^*$) whereas irradiation in the infrared (IR) region leads to vibrational excitations, enabling the measurement of vibrational CD (VCD) spectra.[6]

An ECD spectrum in liquid phase was first recorded by Cotton in 1895, while it took almost a further century until the first VCD measurements were reported.[7,8] The latter was measured by Holzwarth et al. in 1974 and a year later was confirmed independently by Nafie et al.[9,10] For these measurements, crystallization of the sample and the presence of heavy atoms was not required

J. Groß and Dr. J. Kühlborn contributed equally.

anymore. VCD is normally measured for neat liquid or solution samples but can also be measured in the gas phase and in the solid phase.[6]

While the sensitivity of ECD is two orders of magnitude higher compared with VCD (resulting in a smaller amount of the sample being required), the compound of interest needs to have a chromophore close to a stereogenic center or another stereogenic element so that ECD spectroscopy can safely be applied. In contrast, VCD is even suitable for saturated hydrocarbons. In combination with Raman optical activity spectroscopy, these three chiroptical spectroscopies can usefully complement each other and offer specific advantages in the investigation of various stereochemical aspects.[3,6,11–16]

The simulation of VCD spectra requires suitable quantum-mechanical methods to calculate the vibrational rotational strengths. While the magnetic dipole transition moments contribute to them, the calculation is not possible within the Born–Oppenheimer (BO) approximation.[17] In the late 20th century, several ad hoc approaches were proposed (e.g., the fixed partial charge model,[18] a coupled oscillator model,[19] or a localized molecular orbital model[20]) but none of these proved to be generally useful.[21] Stephens reported in 1985 a solution for the calculation of magnetic dipole transition moments of vibrational transitions and subsequently, the first predicted VCD spectra at DFT level in 1994.[17,22] Until today, analytical derivative methods[23,24] in combination with gauge-invariant atomic orbital (GIAO) basis sets are applied for the prediction of vibrational rotational strengths by the calculation of the harmonic force field (HFF), the atomic polar tensors (APTs), and the atomic axial tensors (AATs) in a cost-efficient and accurate manner using DFT.[25–27]

Although visual comparison of measured and calculated VCD curves is often sufficient to decide on the correct AC, a quantitative comparison relies on the use of algorithms and computer programs.[28,29] In 2010, one of the first methods was published by Shen et al. (*Sim*VCD),[30] followed by the freely available software *CDSpecTech* by Covington and Polavarapu[29] and *SpecDis* by Bruhn et al.[3,31] The latter was developed initially for the comparison of experimental and calculated UV and ECD curves but was then extended to cover IR and VCD as well. The similarity factors f and f^* (enantiomeric f) were introduced to quantify the degree of matching of two curves (in this case experimental and calculated IR/VCD spectra) within a given range of wavelengths. Their values reach from 0 to 1, with 1 representing an ideal match. The absolute value of their difference ($|f - f^*|$) of the similarity factors of both enantiomers is called the Δ-value or enantiomeric similarity index (ESI), introduced by Bultinck et al.,[3,32–34] and serves as a useful measure to differentiate between two enantiomers.

The calculation of a sufficient number of excited states is necessary for ECD prediction of the whole range of the experimental spectrum,[3] for which the time-dependent density functional theory (TD-DFT) method may be very cost effective.[35] A computational flowchart was presented by Bruhn et al. for the AC determination by ECD including conformational analysis, optimization of the geometries, solvent effects and Boltzmann weighting.[36] This general procedure can also be adapted to VCD, where the DFT level of theory is sufficient for the calculation of vibrational rotational strengths to simulate the spectra (see the Supporting Information).[25] To achieve more accurate predictions and avoid arbitrary wavenumber shifts, anharmonic corrections at the second-order level of vibrational perturbation theory (VPT2)[37] can be applied, which have been successfully demonstrated for small molecules in recent years.[38,39] By applying the generalized VPT2 approach, Fusè et al. were able to compare experimental IR and VCD spectra with predicted spectra in the range of 900–9000 cm^{-1} including the fundamental and overtone CH-stretching regions and the mid-IR region.[40] Despite the increased computational costs, a perfect match has not yet been accomplished, and most AC determinations of flexible or larger molecules still rely on the calculation of harmonic spectra. Suitable programs for quantum-mechanical calculations are, among others, the Amsterdam Modeling Suite,[41] Dalton,[42] Gaussian,[43] and TURBOMOLE.[44]

The reader should bear in mind that AC determination is still not a black-box method and every computational method is prone to error.[45] For detailed information about the various methods of VCD spectra calculation, the quantum-mechanical theory behind them, MD simulations for the explicit description of solvent effects, and the transfer to machine learning methods, the reader shall be referred to the existing literature.[17,21,25,46–54]

2 | AIM OF THE CONDUCTED RESEARCH

The proposed procedure is analogous to that published by Pescitelli and Bruhn (summarized in Figure 1).[36]

1. A conformational search needs to be performed, ideally on a low-cost computational level (e.g., MMFF[55] or AM1[56]/PM6).[57] The main goal in this step is to obtain as many conformers as possible for a precise description of the conformational ensemble.

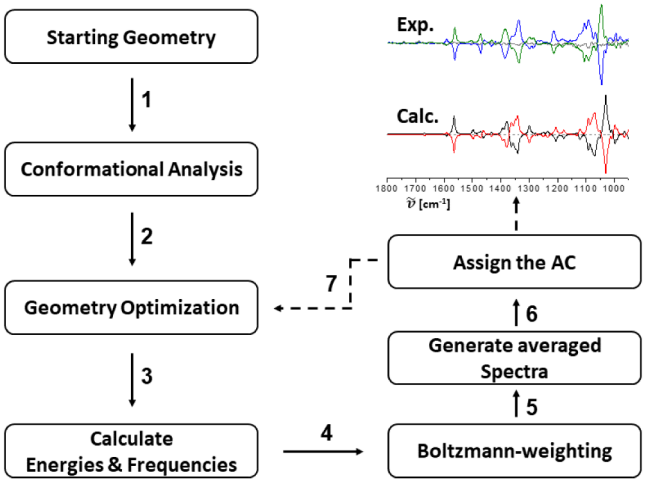

FIGURE 1 Flowchart for the general procedure to enable AC determination by VCD calculations.

2. A geometry optimization for each molecule from the obtained ensemble at DFT level with a given combination of *functional/basis set/solvation model* is the second step. Depending on the computational resources available, either a threshold can be applied to restrict the low-energy conformers, or every conformer can be kept until the Boltzmann weighting (Step 4).
3. Subsequently, an energy and frequency calculation must be performed for the optimized structures with the same method used for the geometry optimization. With the latter, true energy minima for each conformer can be confirmed by frequency analysis. Also, the desired vibrational rotational strengths for the prediction of the spectra are calculated in this step.
4. A Boltzmann weighting based on the calculated energies needs to be performed for the conformer ensemble. This can be either done manually or with suitable programs (e.g., *SpecDis*).
5. Now, the theoretical spectra can be plotted by converting the calculated vibrational frequencies, dipole strengths and rotational strengths into Lorentzian line shape functions.[11,58] Together with the previously obtained population-weighting factors, an averaged and Boltzmann-weighted IR and VCD spectrum can be generated.
6. In the last step, the obtained spectra are compared with the experimental spectra in a given wavelength region. For the best overlap, the scaling factor (to compensate a general frequency shift of the calculated spectra)[58,59] and the band width γ of the Lorentz curves need to be optimized. For both parameters, a range can be set to limit the employed cross-section algorithm (see the Supporting Information for the herein applied settings).[3] To prevent confirmation bias, as the AC is still unknown at this point, these values should be generated based on the comparison of IR-spectra alone and subsequently be applied to the predicted VCD spectrum to quantify the AC determination (e.g., using the ESI value).
7. If insufficient values are obtained, one should choose a different combination of functional and basis set and start over from Step 2 with a new geometry optimization.

In this benchmark analysis, calculations were solely conducted at the DFT level of theory. This approach has the advantage of low computational cost compared with more sophisticated post-HF ab initio approaches. Several classes of functionals, basis sets (Table 1) and two solvation models (IEFPCM[46,60,61] and SMD)[62] were compared to each other (see the Supporting Information for the respective xyz files). To cover a broad range of functionals, hybrid functionals, long-range-corrected functionals, and pure exchange–correlation functionals were taken into account, both with and without dispersion correction. These functionals were combined with several standard Dunning, Pople, and Karlsruhe basis sets (Table 1). For further insights, the reader is kindly referred to existing literature.[63–68]

With this paper, we intend to recommend a general approach on how to determine the AC of a chiral molecule by VCD using the free software *SpecDis* and without having to use too cost-intensive methods.

3 | THE APPROACH

The investigated molecules were selected to ensure clarity and comparability of the results. For the benchmarking analysis, fewer complex structures were chosen to keep the computational cost at a reasonable level. Furthermore, the molecules should have as few conformers as possible (ideally just a single one), contributing to cost-efficiency and reducing potential errors due to missing conformers in this benchmark approach. The solubility in carbon tetrachloride was the topmost criterion for the experimental spectroscopic part because it is a preferred solvent for VCD spectroscopy. Furthermore, carboxylic acids were excluded because they can form dimers in solution which are challenging to incorporate in the theoretical part.[107] Based on these criteria, we chose (1*R*,4*R*)-camphor (**1**), (2′*R*,3′*R*)-caripyrin (**2**), (*R*)-propylene oxide (**3**), (*S*)-1-phenethylamine (**4**), (*R*)-methyl *p*-tolyl sulfoxide (**5**), and (1*R*,4*R*)-thiocamphor (**6**) (Figure 2). Except for the sulfoxide **5**, which was prepared synthetically, all compounds were purchased from commercial sources.

TABLE 1 Chosen functionals and basis sets for the theoretical prediction of IR- and VCD spectra.

Functional		Basis set	
Hybrid	mPW1PW91[69–74]	6-31G[75]	Pople
	B3LYP[22,76–78]	6-31G(d)[75,79,80]	
	PW6B95[81]	6-31G(d,p)[75,79,80]	
	M06-2X[74]	6-31+G(d,p)[75,79,80,82]	
	PBE0[70,83,84]	6-31++G(d,p)[75,79,80,82]	
	B3P86[76,85]	6-311G[86,87]	
	B3PW91[71,72,74,76,88,89]	6-311G(d)[79,80,86,87]	
	TPSSh[89,90]	6-311G(d,p)[79,80,86,87]	
Long-range-corrected	CAM-B3LYP[91]	6-311+G(d,p)[79,80,82,86,87]	
	LC-ωPBE[71–73]	6-311++G(d,p)[79,80,82,86,87]	
	ωB97X-D[92,93]	def2-SVP[94–98]	Karlsruhe
Exchange–correlation (GGA and meta-GGA)	TPSS[99]	def2-TZVP[94–98]	
	PBE[83,84]	def2-TZVPP[94–98]	
	BP86[85]	cc-pVDZ[100,101]	Dunning
	B97-D3[102–105]	cc-pVTZ[100,101]	
		aug-cc-pVTZ[106]	

Note: Thus, a total number of 480 combinations were calculated and checked for similarity for each molecule.

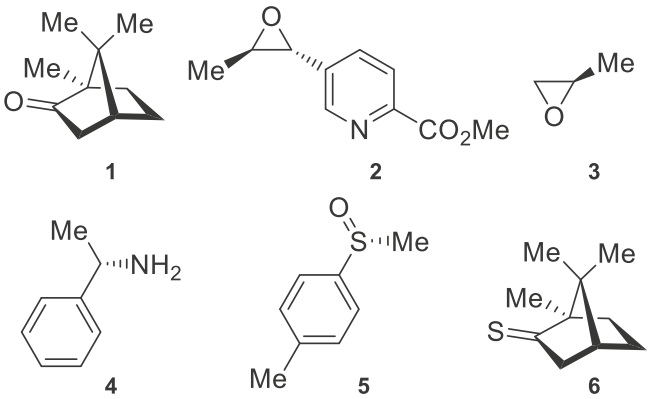

FIGURE 2 Molecular structures and absolute configurations of the examined compounds.

The results were evaluated including all compounds and additionally without the sulfur-containing compounds **5** and **6** because they were expected to behave differently due the presence of a polarizable third-row element. Technical, experimental, and computational details are specified in the Supporting Information, the coordinate files are in an additional zip file and the ESI value was used as the major evaluation criterion. The reader should keep in mind that a low ESI value does not necessarily correspond to a poor qualitative description of the experimental spectrum but can also result from poorly determined fitting parameters (see the Supporting Information). The quality of VCD spectra of flexible molecules also depends on the adequate description of the conformer ensemble in solution and another combination of *functional/basis set/solvation model* may be better suited for the correct description of equilibrium geometries and conformational populations.[14,15]

4 | RESULTS AND DISCUSSION

Sorting the respective levels of theory for the single molecules based on the ESI revealed that there are combinations that produce values higher than 80% for every molecule except for sulfoxide **5**. In those cases, the determination of the AC can be regarded as certain. For sulfoxide **5**, values of higher than 60% were obtained while values higher than 70% were not. This might be due to the aforementioned considerations regarding sulfur combined with the fact that the sulfur itself is the stereocenter of this compound.

5 | EVALUATION OF MEAN VALUES AND STANDARD DEVIATION

The calculation and plot of the mean values and standard deviations of the respective ESI values for every combination of *functional/basis set/solvation model* examined displays a common issue of DFT methods (Figure 3). About

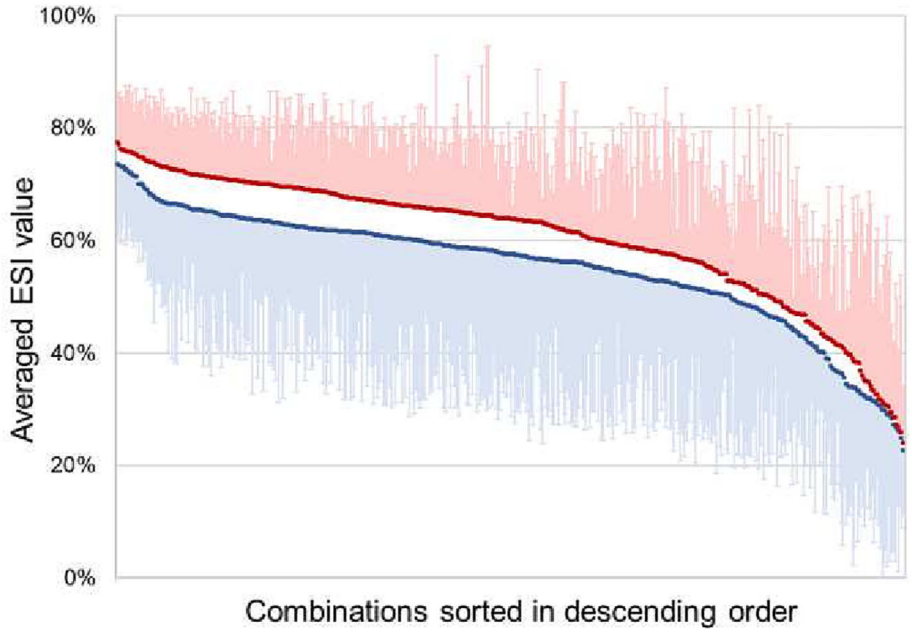

FIGURE 3 Averaged ESI values and standard deviations for all compounds (blue) and excluding the sulfur-containing compounds (red), sorted by mean values in descending order. For the sake of clarity, the standard deviation is only printed in one direction.

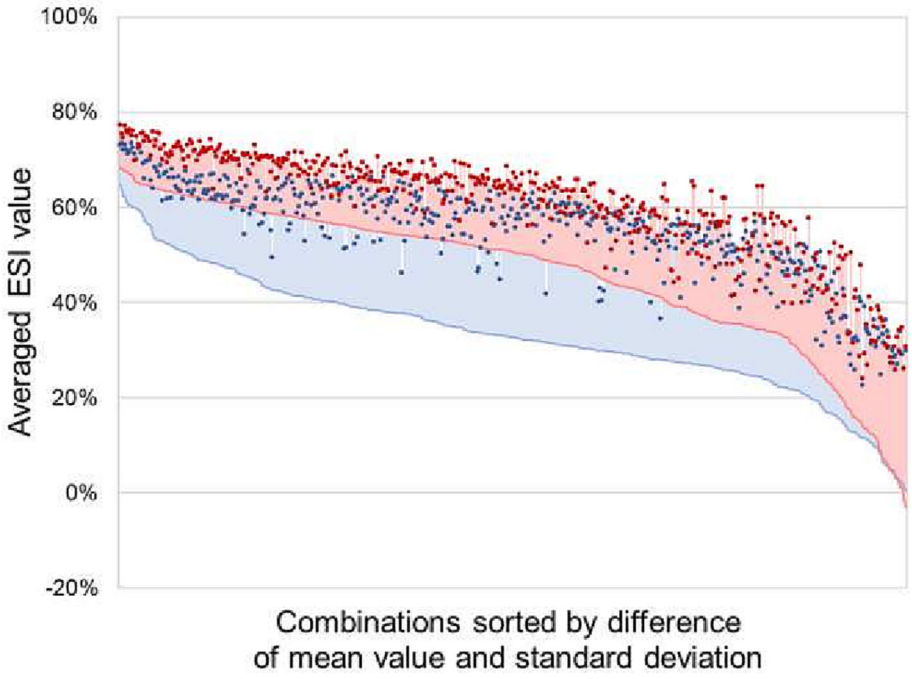

FIGURE 4 The averaged ESI values sorted by the difference of the mean value and the respective standard deviation in descending order, for all compounds (blue) and molecule **1**–**4**. The standard deviation is only printed in one direction to indicate the lower limitation.

50% of them produces quite high averaged ESI values of around 50% or higher but the deviation is also relatively high, especially in the case where all molecules were included (blue data set). An overall higher averaged ESI is achieved when only the molecules devoid of sulfur were evaluated (red data set), indicating a higher accuracy for light atom structures. The highest average values for a single combination reached in this work were above 70% (see the Supporting Information). In detail, there are 14 combinations that are above this threshold and it is striking that among these, the only basis sets represented are Dunning's correlation consistent (cc) triple zeta basis sets cc-pVTZ and aug-cc-pVTZ.[100,101,106] The most frequently occurring functionals were either hybrid (seven times) or long-range corrected functionals (six times), but there is no trend regarding the solvation model observable. When the sulfur-containing compounds **5** and **6** are not considered, the top 13 combinations reach averaged ESI values above 75%, this time including Pople, redefined Karlsruhe and Dunning basis sets, four, four, and five times, respectively. Among these 13, there is four times the B3LYP,[22,76–78] three times the Coulomb-

attenuated extended CAM-B3LYP,[91] and six times the ωB97X-D[92,93] functional. This supports the finding of the overall good performance of hybrid and long-range corrected functionals. A similar effect has been observed by Tsuneda and Hirao for the reproducibility of van der Waals bonds and the calculation of oscillator strengths in time-dependent DFT calculations using the latter class of functionals.[108]

When computing and plotting the difference between mean values and standard deviation (Figure 4), the lower limitations of the combinations are revealed (blue: all molecules, red: excluding sulfur). If the sulfur-containing molecules are excluded, a higher precision of the averaged ESI values is observable. In general, the plotted lower limitation lines show a relatively flat trend until reaching the negative spikes on the right edge of the graph. This again shows that DFT methods have a reasonable performance on average. Notably, those negative spikes (blue and red) almost exclusively contain the widely applicated Pople basis sets (without any additional polarization or diffuse functions)[75,86,87] which is also true for the graph in Figure 3, albeit to a lesser extent (see the Supporting Information).

It is noteworthy that one of the most frequently used combinations (B3LYP/6-311G(d,p)/SMD)[22,62,76–80,86,87] ranks second in this evaluation (just first and second row elements).

6 | EVALUATION OF THE 100 TOP AND BOTTOM COMBINATIONS

Extending this statistical approach to the top 100 and bottom 100 combinations sorted by the mean values of the ESI and the difference between them and the standard deviation (Figure 5) gives a more general trend of how these perform in VCD calculation (the bottom 100 combinations are displayed in the Supporting Information).

7 | FUNCTIONALS

Regarding the functionals (Figure 5, top), the first thing to notice is that they appear similarly often in the same plotted categories, regardless of whether sulfur is included or not. The combinations using B3P86,[76,85]

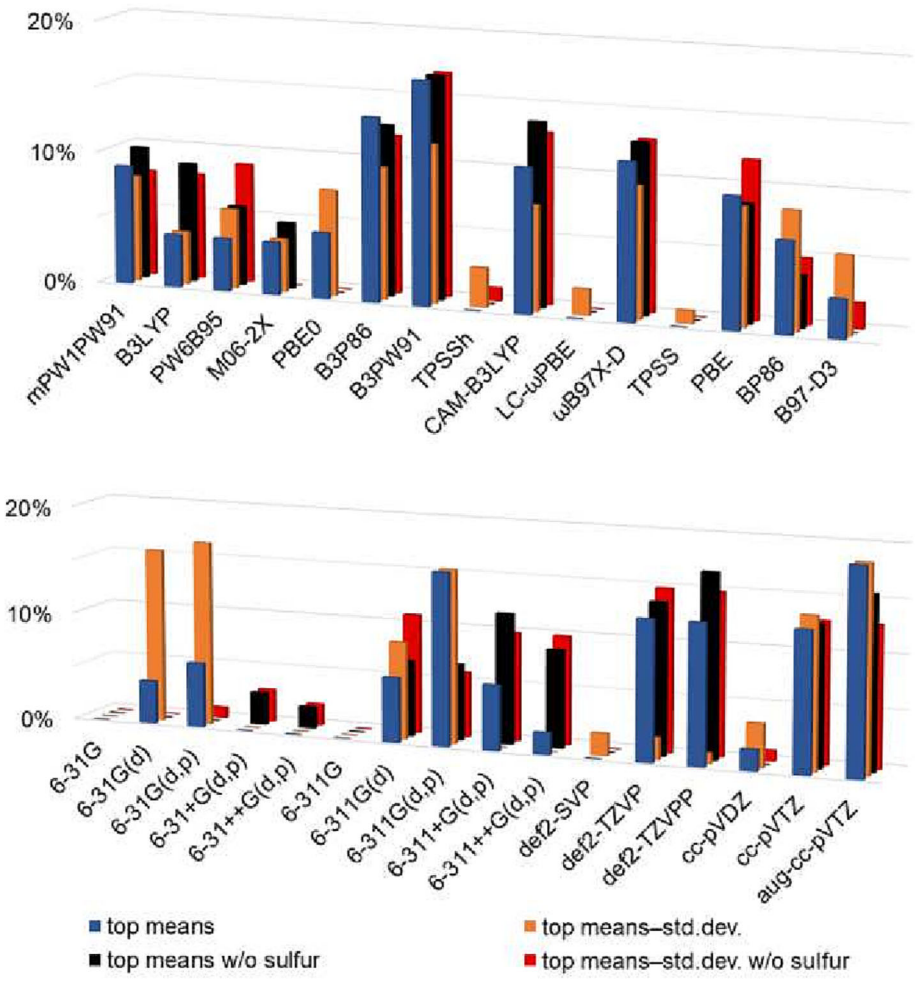

FIGURE 5 Occurrence of the respective examined functionals (top) and basis sets (bottom) among the top 100 combinations sorted by mean values and difference between mean value and standard deviation. The results were evaluated with and without the sulfur-containing compounds.

B3PW91,[71,72,74,76,88,89] and ωB97X-D[92,93] are the most frequent among the top 100 combinations and in the case where the difference between the mean value and the standard deviation is investigated (blue and orange bar). For the previous two functionals, this finding is in accordance with the studies of Ravichandran and Banik, who obtained similar results by benchmarking the potential of DFT methods to calculated vibrational frequencies (just IR), but it should be noted that the authors did not investigate the influence of different basis sets or a solvation model.[109] Barone et al. also reported on the good results that can be obtained with ωB97X-D functional in conjunction with double-ζ basis sets, after the authors benchmarked, among others, the equilibrium geometry and harmonic vibrational properties of 10 organic molecules of atmospheric and astrochemical relevance and compared the results with experimental values or high-level CCSD(T) computations.[110]

In the hybrid functional class, mPW1PW91[69–74] is the next most frequent among the top 100 combinations, while TPSSh[57,58] is the least. The other functionals are represented more or less equally in the top 100 and bottom 100 combinations. These results align with the extensive investigations of Goerigk and Grimme, who studied the performance of DFT methods regarding the calculation of thermochemistry, kinetics, and noncovalent interactions and came to the conclusion that hybrid functionals only had a medium performance.[111]

The range-separated functional CAM-B3LYP[91] performs quite well, whereas the remaining investigated functional from this class (LC-ωPBE[71–73]) is the most frequent among the bottom 100 combinations. Regarding the class of GGA and mGGA functionals, PBE[57,58] and BP86[85] appear quite often in the top 100, B97-D3[102–105] shows a balanced performance, and TPSS[99] appears the second most frequent among the bottom 100.

8 | BASIS SETS

In terms of the basis sets examined (Figure 5, bottom), the large Dunning basis sets perform quite well and occur the most amidst the top 100. The Karlsruhe basis sets (def2-TZVP and def2-TZVPP)[94–98] behave similarly. The smaller basis sets of the two previous classes, cc-pVDZ[74,75] and def2-SVP,[94–98] as well as the Pople basis sets 6-31G[75] and 6-311G[86,87] are found most often among the bottom 100 in both cases. This might be due to the fact that these basis sets consist of too few basis functions to describe the system sufficiently.

Regarding the other Pople basis sets, 6-311G(d,p)[79,80,86,87] performs quite well when all molecules are taken into account (blue bars). If sulfur is excluded, 6-311+G(d,p) and 6-311++G(d,p)[79,80,82,86,87] have the highest share among the top 100 combinations (black bars).

9 | SOLVATION MODELS

In terms of the solvation model, it does not seem to make a difference whether the model based on density (SMD)[62] or the integral equation formalism model polarizable continuum model (IEFPCM)[46,60,61] is used (see the Supporting Information).

10 | EVALUATION OF THE BEST PERFORMING COMBINATIONS FOR SINGLE COMPOUNDS

As already mentioned, there are several combinations that reached ESI values higher than 80% for every compound except for the sulfoxide (**5**). Only two combinations could exceed the aforementioned barrier for three molecules, each time using the ωB97X-D[92,93] functional and the SMD[62] solvation model, in conjunction with the 6-311+G(d,p)[79,80,82,86,87] and the aug-cc-pVTZ basis set.[106] The occurrence of a single combination (blue bars) and when a combination achieved for two molecules an ESI higher than 80% (orange bars), as well as the corresponding evaluation where the sulfur-containing compound **6** was excluded, were plotted (grey and yellow bars). Regarding the distribution of functionals and basis sets among these combinations (Figure 6), there are similarities and differences compared with the previous considerations.

11 | FUNCTIONALS

The functionals that reached >80% ESI for one compound (blue and grey bars) are more or less equally distributed (Figure 6, top), while mPW1PW91,[69–74] PBE0,[70,83,84] and ωB97X-D[92,93] being most frequent. Regarding the occurrence for two molecules, M06-2X,[74] B3P86,[76,85] and ωB97X-D[92,93] perform the best when all molecules are considered (orange bars), whereas B3LYP[22,76–78] and ωB97X-D[92,93] stand out when thiocamphor (**6**) is excluded (yellow bars). These findings are in accordance with the previously made observations that hybrid and long-range-corrected functionals can show a good performance, whereas the hybrid version (TPSSh[89,90]) and the meta-GGA functional TPSS[99] are again among the least frequent.

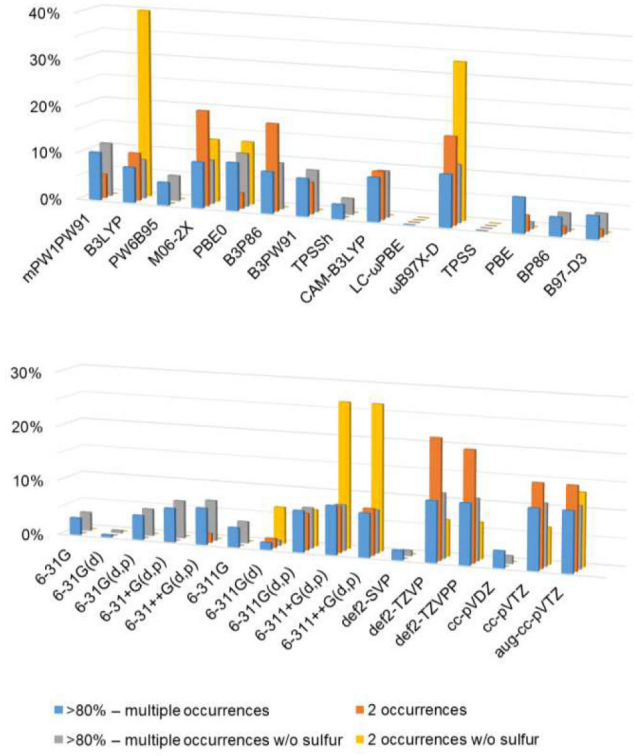

FIGURE 6 Occurrence of the respective examined functionals (top) and basis sets (bottom) among the combinations that reached over 80% ESI for at least one specific compound.

Nevertheless, the subpar performance of LC-ωPBE[71–73] on the other hand is rather surprising, but it was also among the less frequent functionals in the previous evaluation (vide supra).

12 | BASIS SETS

In terms of the basis sets (Figure 6, bottom), the occurrence in a single combination is almost independent on whether sulfur is included or not (blue and grey bars), comparable to the behavior of the functionals. Again, the Dunning (cc-pVTZ and aug-cc-pVTZ)[100,101,106] and Karlsruhe basis sets (def2-TZVP and def2-TZVPP)[94–98] are well represented but once more without cc-pVDZ[100,101] and def2-SVP.[94–98] The four basis sets mentioned foremost are also the most frequent amidst those combinations that reached at least 80% ESI for two compounds (orange bar). If sulfur is excluded, the Pople basis sets 6-311+G(d,p) and 6-311++G(d,p)[79,80,82,86,87] show the highest occurrence (yellow bar). The overall outstanding performance of the two triple zeta Dunning basis sets in combination with DFT functionals should be emphasized because these basis sets were originally developed using configuration interaction (CI) methods.[100] Nevertheless, this indicates that moving from double zeta (in the case of the Dunning basis sets) and split valence (in the case of the Ahlrichs basis sets) to the respective triple zeta basis sets gives a significant improvement of the results.

Regarding the Pople basis sets, there is a similar trend observable as previously, where smaller basis sets are less frequent among the high ESI values, especially when the occurrence for two molecules of the test set is investigated. In fact, it is clearly indicated that going from split valence double to triple zeta and adding diffuse functions gradually increases the accuracy because these basis sets become more frequent (blue and grey bars).

13 | SOLVATION MODELS

Again, the choice of the solvation model does not seem to make a crucial difference (a graphical representation can be found in the Supporting Information). Continuum models consider isotropic solvents, to which carbon tetrachloride approximately belongs, whereas SMD is a more universal solvation model and offers specifically parameterized radii to construct the solute cavity. Ultimately, both SMD[62] and IEFPCM[46,60,61] solve the Poisson–Boltzmann equation similarly.[62]

14 | EVALUATION BY SINGLE COMPOUNDS

Unsurprisingly, the methods that performed well for caripyrin (**2**) and propylene oxide (**3**) are very similar. Among these two, there is a high share of the B3LYP[22,76–78] functional with triple zeta basis sets (Pople, Karlsruhe, and Dunning equally distributed). Surprisingly, there is exclusively the SMD[62] solvation model being present.

The combinations that worked well on camphor (**1**) and thiocamphor (**6**) are almost identical but they differ completely from the ones of caripyrin (**2**) and propylene oxide (**3**). Interestingly, some of these methods (M06-2X,[74] PBE0,[70,83,84] and ωB97X-D[92,93]) in conjunction with larger Pople basis sets also performed well for phenethylamine (**4**), although these compounds differ significantly in their structure. In this case, almost only the IEFPCM[46,60,61] solvation model was present. Moreover, camphor (**1**), thiocamphor (**6**), and phenethylamine (**4**) were the only molecules where the two combinations already mentioned could achieve ESI values above 80% for all three molecules (vide supra).

After filtering these methods by their computational requirements to single out accurate but also cost-efficient methods which can also be applied to larger molecules,

we obtain the following list which could serve as starting point for the elucidation of the AC applying VCD spectroscopy:

- Chiral epoxides: B3LYP/6-311+G(d,p)/SMD.
- Bicyclic (thio)ketone or chiral amine: M06-2X/6-311+G(d,p)/IEFPCM, PBE0/6-311G(d)/IEFPCM, and ωB97X-D/6-311+G(d,p)/IEFPCM.

If sulfur-containing molecules give insufficient results, higher order polarization functions may be necessary, as described by Scholten et al.[112] The good performance of the PBE0 functional[70,83,84] is surprising because it is one of the few parameter-free functionals. Despite the overall good performance of the triple zeta Dunning and Ahlrichs basis sets, they are not included in the foregoing list due to their reduced cost-efficiency.

15 | CONCLUSION

The present work shows that there is no single combination to recommend in terms of the calculation of VCD spectra which is a common phenomenon of DFT methods. This leads to the outcome that there is no "one size fits all" multi-purpose method. However, based on the results of this study combined with our experience in successful calculation of VCD spectra and AC determination, some general advice can be given. In any case, it is always recommended to validate the results by simulating the VCD spectra with a different combination of *functional/basis set/solvation model* to exclude misassignments. Additional chiroptical methods, X-ray crystallography, or further measures, such as the confidence level, statistical robustness, or the vibrational dissymmetry factor, can also be applied to support the reliability of the AC assignment.[34,113,114]

- For the conformer distribution of larger molecules, force field, semi-empiric, or cost-efficient DFT methods are advised. Subsequent confinement of the conformer ensemble based on the relative energy might be useful.
- GGA and meta-GGA functionals are disadvantageous while hybrid and range-separated functionals are favored.
- Combinations worth trying are:
  - B3LYP/6-311G(d,p)/SMD
  - ωB97X-D/6-311+G(d,p)/SMD
  - M06-2X/6-311+G(d,p)/IEFPCM
  - PBE0/6-311G(d)/IEFPCM.

The Opatz group has particularly good experience with the hybrid density functionals B3LYP[22,76–78] and B3PW91[71,72,74,76,88,89] combined with the Pople basis set 6-311G(d,p)[79,80,86,87] and the IEFPCM[46,60,61] solvation model in the determination of the AC of natural products (e.g., dioxolanones,[115] hymenosetin,[116] caripyrin,[117] and oxalicumone C[118]), pesticides (imazalil),[119] synthetic cannabinoids (MDMB-CHMCZCA),[120] and synthetic products (e.g., 2,3-dihydro-1*H*,5*H*-pyrazolo[1,2-*a*]pyrazoles,[121] an oxazinone derivative,[122] and cyclopenta[*b*]benzofurans[123]).

ACKNOWLEDGMENTS

Parts of this research were conducted using the supercomputer MOGON 2 offered by Johannes Gutenberg-University Mainz (hpc.uni-mainz.de), which is a member of the Alliance for High Performance Computing in Rhineland-Palatinate (AHRP, www.ahrp.info) and the Gauss Alliance e.V. The authors gratefully acknowledge the computing time granted on the supercomputer MOGON 2 at Johannes Gutenberg-University Mainz (hpc.uni-mainz.de). Open Access funding enabled and organized by Projekt DEAL.

DATA AVAILABILITY STATEMENT

The data that support the findings of this study are available in the Supporting Information of this article.

ORCID

Till Opatz https://orcid.org/0000-0002-3266-4050

REFERENCES

1. van't Hoff JH. *La chimie dans l'espace*. Bazendijk; 1875.
2. Bijvoet JM, Peerdeman AF, van Bommel AJ. Determination of the absolute configuration of optically active compounds by means of X-rays. *Nature*. 1951;168(4268):271-272. doi:10.1038/168271a0
3. Bruhn T, Schaumlöffel A, Hemberger Y, Bringmann G. SpecDis: quantifying the comparison of calculated and experimental electronic circular dichroism spectra. *Chirality*. 2013;25(4):243-249. doi:10.1002/chir.22138
4. He Y, Bo W, Dukor RK, Nafie LA. Determination of absolute configuration of chiral molecules using vibrational optical activity: a review. *Appl Spectrosc*. 2011;65(7):699-723. doi:10.1366/11-06321
5. Stephens PJ, Devlin FJ, Pan J-J. The determination of the absolute configurations of chiral molecules using vibrational circular dichroism (VCD) spectroscopy. *Chirality*. 2008;20(5):643-663. doi:10.1002/chir.20477
6. Nafie LA. *Vibrational Optical Activity: Principles and Applications*. John Wiley & Sons; 2011.
7. Cotton A. Dispersion rotatoire anomale des corps absorbants. *Compt Rend*. 1895;120:1044.
8. Crabbé P. *Optical Rotatory Dispersion and Circular Dichroism in Organic Chemistry*. Holden-Day; 1965.
9. Holzwarth G, Hsu EC, Mosher HS, Faulkner TR, Moscowitz A. Infrared circular dichroism of carbon-hydrogen

and carbon-deuterium stretching modes. Observations. *J Am Chem Soc*. 1974;96(1):251-252. doi:10.1021/ja00808a042

10. Nafie LA, Cheng JC, Stephens PJ. Vibrational circular dichroism of 2,2,2-trifluoro-1-phenylethanol. *J Am Chem Soc*. 1975; 97(13):3842-3843. doi:10.1021/ja00846a061
11. Berova N, Polavarapu PL, Nakanishi K, Woody RW. *Comprehensive Chiroptical Spectroscopy: Instrumentation, Methodologies, and Theoretical Simulations*. John Wiley & Sons; 2011.
12. Berova N, Polavarapu PL, Nakanishi K, Woody RW. *Comprehensive Chiroptical Spectroscopy, Volume 2: Applications in Stereochemical Analysis of Synthetic Compounds, Natural Products, and Biomolecules*. John Wiley & Sons; 2012.
13. Polavarapu PL. Renaissance in chiroptical spectroscopic methods for molecular structure determination. *Chem Record*. 2007;7(2):125-136. doi:10.1002/tcr.20117
14. Batista JM Jr, Blanch EW, Bolzani VS. Recent advances in the use of vibrational chiroptical spectroscopic methods for stereochemical characterization of natural products. *Nat Prod Rep*. 2015;32(9):1280-1302. doi:10.1039/C5NP00027K
15. Polavarapu PL, Santoro E. Vibrational optical activity for structural characterization of natural products. *Nat Prod Rep*. 2020;37(12):1661-1699. doi:10.1039/D0NP00025F
16. Merten C, Golub TP, Kreienborg NM. Absolute configurations of synthetic molecular scaffolds from vibrational CD spectroscopy. *J Org Chem*. 2019;84(14):8797-8814. doi:10.1021/acs.joc.9b00466
17. Stephens PJ. Theory of vibrational circular dichroism. *J Phys Chem*. 1985;89(5):748-752. doi:10.1021/j100251a006
18. Schellman JA. Vibrational optical activity. *J Chem Phys*. 1973; 58(7):2882-2886. doi:10.1063/1.1679592
19. Holzwarth G, Chabay I. Optical activity of vibrational transitions: a coupled oscillator model. *J Chem Phys*. 1972;57(4): 1632-1635. doi:10.1063/1.1678447
20. Nafie LA, Walnut TH. Vibrational circular dichroism theory: a localized molecular orbital model. *Chem Phys Lett*. 1977; 49(3):441-446. doi:10.1016/0009-2614(77)87010-3
21. Stephens PJ, Lowe MA. Vibrational circular dichroism. *Annu Rev Phys Chem*. 1985;36(1):213-241. doi:10.1146/annurev.pc.36.100185.001241
22. Stephens PJ, Devlin FJ, Chabalowski CF, Frisch MJ. Ab initio calculation of vibrational absorption and circular dichroism spectra using density functional force fields. *J Phys Chem*. 1994;98(45):11623-11627. doi:10.1021/j100096a001
23. Amos RD. *Molecular property derivatives*. Ab Initio Methods in Quantum Chemistry, Volume 67, Part 1. Wiley; 2009:99.
24. Pulay P. Analytical derivative methods in quantum chemistry. *Adv Chem Phys*. 1987;69:241-286. doi:10.1002/9780470142943.ch4
25. Stephens PJ. Gauge dependence of vibrational magnetic dipole transition moments and rotational strengths. *J Phys Chem*. 1987;91(7):1712-1715. doi:10.1021/j100291a009
26. Cheeseman JR, Frisch MJ, Devlin FJ, Stephens PJ. Ab initio calculation of atomic axial tensors and vibrational rotational strengths using density functional theory. *Chem Phys Lett*. 1996;252(3):211-220. doi:10.1016/0009-2614(96)00154-6
27. Crawford TD. Ab initio calculation of molecular chiroptical properties. *Theor Chem Acc*. 2006;115(4):227-245. doi:10.1007/s00214-005-0001-4
28. Polavarapu PL, Covington CL. Comparison of experimental and calculated chiroptical spectra for chiral molecular structure determination. *Chirality*. 2014;26(9):539-552. doi:10.1002/chir.22316
29. Covington CL, Polavarapu PL. CDSpecTech: a single software suite for multiple chiroptical spectroscopic analyses. *Chirality*. 2017;29(5):178-192. doi:10.1002/chir.22691
30. Shen J, Zhu C, Reiling S, Vaz R. A novel computational method for comparing vibrational circular dichroism spectra. *Spectrochim Acta A Mol Biomol Spectrosc*. 2010;76(3):418-422. doi:10.1016/j.saa.2010.04.014
31. Bruhn T, Schaumlöffel A, Hemberger Y, Pescitelli G. *SpecDis, Version 1.71*; 2017. https://specdis-software.jimdofree.com/
32. Bruhn T, Schaumlöffel A, Hemberger Y, Bringmann G. *SpecDis Version 1.61*. University of Wuerzburg; 2013.
33. Kuppens T, Langenaeker W, Tollenaere JP, Bultinck P. Determination of the stereochemistry of 3-hydroxymethyl-2,-3-dihydro-[1,4]dioxino[2,3-*b*]-pyridine by vibrational circular dichroism and the effect of DFT integration grids. *J Phys Chem A*. 2003;107(4):542-553. doi:10.1021/jp021822g
34. Debie E, De Gussem E, Dukor RK, Herrebout W, Nafie LA, Bultinck P. A confidence level algorithm for the determination of absolute configuration using vibrational circular dichroism or Raman optical activity. *ChemPhysChem*. 2011; 12(8):1542-1549. doi:10.1002/cphc.201100050
35. Autschbach J, Nitsch-Velasquez L, Rudolph M. Time-dependent density functional response theory for electronic chiroptical properties of chiral molecules. In: Naaman R, Beratan DN, Waldeck D, eds. *Electronic and Magnetic Properties of Chiral Molecules and Supramolecular Architectures*. Springer; 2011:1-98.
36. Pescitelli G, Bruhn T. Good computational practice in the assignment of absolute configurations by TDDFT calculations of ECD spectra. *Chirality*. 2016;28(6):466-474. doi:10.1002/chir.22600
37. Bloino J, Barone V. A second-order perturbation theory route to vibrational averages and transition properties of molecules: general formulation and application to infrared and vibrational circular dichroism spectroscopies. *J Chem Phys*. 2012; 136(12):124108. doi:10.1063/1.3695210
38. Kreienborg NM, Bloino J, Osowski T, Pollok CH, Merten C. The vibrational CD spectra of propylene oxide in liquid xenon: a proof-of-principle CryoVCD study that challenges theory. *Phys Chem Chem Phys*. 2019;21(12):6582-6587. doi:10.1039/C9CP00537D
39. Paoloni L, Mazzeo G, Longhi G, et al. Toward fully unsupervised anharmonic computations complementing experiment for robust and reliable assignment and interpretation of IR and VCD spectra from mid-IR to NIR: the case of 2,3-butanediol and trans-1,2-cyclohexanediol. *J Phys Chem A*. 2020;124(5):1011-1024. doi:10.1021/acs.jpca.9b11025
40. Fusè M, Longhi G, Mazzeo G, et al. Anharmonic aspects in vibrational circular dichroism spectra from 900 to 9000 cm^{-1} for methyloxirane and methylthiirane. *J Phys Chem A*. 2022; 126(38):6719-6733. doi:10.1021/acs.jpca.2c05332
41. Koenis MAJ, Visser O, Visscher L, Buma WJ, Nicu VP. GUI implementation of VCDtools, a program to analyze computed vibrational circular dichroism spectra. *J Chem Inf Model*. 2020;60(1):259-267. doi:10.1021/acs.jcim.9b00956

42. Aidas K, Angeli C, Bak KL, et al. The Dalton quantum chemistry program system. *WIREs Comput Mol Sci*. 2014;4(3):269-284. doi:10.1002/wcms.1172
43. Frisch MJ, Trucks GW, Schlegel HB, et al. *Gaussian 16, Revision A.03*. Gaussian, Inc.; 2016.
44. TURBOMOLE V7.7. Germany: University of Karlsruhe and Forschungszentrum Karlsruhe GmbH, 1989-2007, TURBOMOLE GmbH, since 2007; 2022.
45. Polavarapu PL. Molecular structure determination using chiroptical spectroscopy: where we may go wrong? *Chirality*. 2012;24(11):909-920. doi:10.1002/chir.22015
46. Mennucci B, Cammi R. *Continuum Solvation Models in Chemical Physics: From Theory to Applications*. John Wiley & Sons; 2007. doi:10.1002/9780470515235
47. Sadlej J, Dobrowolski JC, Rode JE. VCD spectroscopy as a novel probe for chirality transfer in molecular interactions. *Chem Soc Rev*. 2010;39(5):1478-1488. doi:10.1039/B915178H
48. Bloino J, Biczysko M, Barone V. Anharmonic effects on vibrational spectra intensities: infrared, Raman, vibrational circular dichroism, and Raman optical activity. *J Phys Chem A*. 2015;119(49):11862-11874. doi:10.1021/acs.jpca.5b10067
49. Yang Q, Mendolicchio M, Barone V, Bloino J. Accuracy and reliability in the simulation of vibrational spectra: a comprehensive benchmark of energies and intensities issuing from generalized vibrational perturbation theory to second order (GVPT2). *Front Astron Space Sci*. 2021;8:665232. doi:10.3389/fspas.2021.665232
50. Vermeyen T, Brence J, Van Echelpoel R, et al. Exploring machine learning methods for absolute configuration determination with vibrational circular dichroism. *Phys Chem Chem Phys*. 2021;23(35):19781-19789. doi:10.1039/D1CP02428K
51. Merten C. Recent advances in the application of vibrational circular dichroism spectroscopy for the characterization of asymmetric catalysts. *Eur J Org Chem*. 2020;2020(37):5892-5900. doi:10.1002/ejoc.202000876
52. Ghidinelli S, Abbate S, Koshoubu J, Araki Y, Wada T, Longhi G. Solvent effects and aggregation phenomena studied by vibrational optical activity and molecular dynamics: the case of pantolactone. *J Phys Chem B*. 2020;124(22):4512-4526. doi:10.1021/acs.jpcb.0c01483
53. Le Barbu-Debus K, Bowles J, Jähnigen S, et al. Assessing cluster models of solvation for the description of vibrational circular dichroism spectra: synergy between static and dynamic approaches. *Phys Chem Chem Phys*. 2020;22(45):26047-26068. doi:10.1039/D0CP03869E
54. Keiderling TA. Instrumentation for vibrational circular dichroism spectroscopy: method comparison and newer developments. *Molecules*. 2018;23(9):2404. doi:10.3390/molecules23092404
55. Halgren TA. Merck molecular force field. I. Basis, form, scope, parameterization, and performance of MMFF94. *J Comput Chem*. 1996;17(5–6):490-519. doi:10.1002/(SICI)1096-987X(199604)17:5/63.0.CO;2-P
56. Dewar MJS, Zoebisch EG, Healy EF, Stewart JJP. Development and use of quantum mechanical molecular models. 76. AM1: a new general purpose quantum mechanical molecular model. *J Am Chem Soc*. 1985;107(13):3902-3909. doi:10.1021/ja00299a024
57. Stewart JJP. Optimization of parameters for semiempirical methods V: modification of NDDO approximations and application to 70 elements. *J Mol Model*. 2007;13(12):1173-1213. doi:10.1007/s00894-007-0233-4
58. Stephens PJ, Devlin FJ, Cheeseman JR. *VCD spectroscopy for organic chemists*. CRC Press; 2012. doi:10.1201/b12278
59. Merrick JP, Moran D, Radom L. An evaluation of harmonic vibrational frequency scale factors. *J Phys Chem A*. 2007;111(45):11683-11700. doi:10.1021/jp073974n
60. Mennucci B, Cancès E, Tomasi J. Evaluation of solvent effects in isotropic and anisotropic dielectrics and in ionic solutions with a unified integral equation method: theoretical bases, computational implementation, and numerical applications. *J Phys Chem B*. 1997;101(49):10506-10517. doi:10.1021/jp971959k
61. Tomasi J, Mennucci B, Cancès E. The IEF version of the PCM solvation method: an overview of a new method addressed to study molecular solutes at the QM ab initio level. *J Mol Struct (THEOCHEM)*. 1999;464(1–3):211-226. doi:10.1016/S0166-1280(98)00553-3
62. Marenich AV, Cramer CJ, Truhlar DG. Universal solvation model based on solute electron density and on a continuum model of the solvent defined by the bulk dielectric constant and atomic surface tensions. *J Phys Chem B*. 2009;113(18):6378-6396. doi:10.1021/jp810292n
63. Goerigk L, Grimme S. Double-hybrid density functionals. *WIREs Comput Mol Sci*. 2014;4(6):576-600. doi:10.1002/wcms.1193
64. Hill JG. Gaussian basis sets for molecular applications. *Int J Quantum Chem*. 2013;113(1):21-34. doi:10.1002/qua.24355
65. Jensen F. Atomic orbital basis sets. *WIREs Comput Mol Sci*. 2013;3(3):273-295. doi:10.1002/wcms.1123
66. Kryachko ES, Ludeña EV. Density functional theory: foundations reviewed. *Phys Rep*. 2014;544(2):123-239. doi:10.1016/j.physrep.2014.06.002
67. Laskowski R, Blaha P, Tran F. Assessment of DFT functionals with NMR chemical shifts. *Phys Rev B*. 2013;87(19):195130. doi:10.1103/PhysRevB.87.195130
68. Laurent AD, Jacquemin D. TD-DFT benchmarks: a review. *Int J Quantum Chem*. 2013;113(17):2019-2039. doi:10.1002/qua.24438
69. Adamo C, Barone V. Exchange functionals with improved long-range behavior and adiabatic connection methods without adjustable parameters: the mPW and mPW1PW models. *J Chem Phys*. 1998;108(2):664-675. doi:10.1063/1.475428
70. Adamo C, Barone V. Toward reliable density functional methods without adjustable parameters: the PBE0 model. *J Chem Phys*. 1999;110(13):6158-6170. doi:10.1063/1.478522
71. Vydrov OA, Heyd J, Krukau AV, Scuseria GE. Importance of short-range versus long-range Hartree-Fock exchange for the performance of hybrid density functionals. *J Chem Phys*. 2006;125(7):074106. doi:10.1063/1.2244560
72. Vydrov OA, Scuseria GE. Assessment of a long-range corrected hybrid functional. *J Chem Phys*. 2006;125(23):234109. doi:10.1063/1.2409292
73. Vydrov OA, Scuseria GE, Perdew JP. Tests of functionals for systems with fractional electron number. *J Chem Phys*. 2007;126(15):154109. doi:10.1063/1.2723119

74. Zhao Y, Truhlar DG. The M06 suite of density functionals for main group thermochemistry, thermochemical kinetics, noncovalent interactions, excited states, and transition elements: two new functionals and systematic testing of four M06-class functionals and 12 other functionals. *Theor Chem Acc*. 2008; 120(1):215-241. doi:10.1007/s00214-007-0310-x
75. Hehre WJ, Ditchfield R, Pople JA. Self-consistent molecular orbital methods. XII. Further extensions of Gaussian-type basis sets for use in molecular orbital studies of organic molecules. *J Chem Phys*. 1972;56(5):2257-2261. doi:10.1063/1.1677527
76. Becke AD. Density-functional thermochemistry. III. The role of exact exchange. *J Chem Phys*. 1993;98(7):5648-5652. doi:10.1063/1.464913
77. Lee C, Yang W, Parr RG. Development of the Colle-Salvetti correlation-energy formula into a functional of the electron density. *Phys Rev B*. 1988;37(2):785-789. doi:10.1103/PhysRevB.37.785
78. Vosko SH, Wilk L, Nusair M. Accurate spin-dependent electron liquid correlation energies for local spin density calculations: a critical analysis. *Can J Phys*. 1980;58(8):1200-1211. doi:10.1139/p80-159
79. Francl MM, Pietro WJ, Hehre WJ, et al. Self-consistent molecular orbital methods. XXIII. A polarization-type basis set for second-row elements. *J Chem Phys*. 1982;77(7):3654-3665. doi:10.1063/1.444267
80. Hariharan PC, Pople JA. The influence of polarization functions on molecular orbital hydrogenation energies. *Theor Chim Acta*. 1973;28(3):213-222. doi:10.1007/BF00533485
81. Zhao Y, Truhlar DG. Design of density functionals that are broadly accurate for thermochemistry, thermochemical kinetics, and nonbonded interactions. *J Phys Chem A*. 2005; 109(25):5656-5667. doi:10.1021/jp050536c
82. Clark T, Chandrasekhar J, Spitznagel GW, Schleyer PR. Efficient diffuse function-augmented basis sets for anion calculations. III. The 3-21+G basis set for first-row elements, Li–F. *J Comput Chem*. 1983;4(3):294-301. doi:10.1002/jcc.540040303
83. Perdew JP, Burke K, Ernzerhof M. Generalized gradient approximation made simple. *Phys Rev Lett*. 1996;77(18):3865-3868. doi:10.1103/PhysRevLett.77.3865
84. Perdew JP, Burke K, Ernzerhof M. Generalized gradient approximation made simple [Phys. Rev. Lett. 77, 3865 (1996)]. *Phys Rev Lett*. 1997;78(7):1396. doi:10.1103/PhysRevLett.78.1396
85. Perdew JP. Density-functional approximation for the correlation energy of the inhomogeneous electron gas. *Phys Rev B*. 1986;33(12):8822-8824. doi:10.1103/PhysRevB.33.8822
86. Krishnan R, Binkley JS, Seeger R, Pople JA. Self-consistent molecular orbital methods. XX. A basis set for correlated wave functions. *J Chem Phys*. 1980;72(1):650-654. doi:10.1063/1.438955
87. McLean AD, Chandler GS. Contracted Gaussian basis sets for molecular calculations. I. Second row atoms, Z=11–18. *J Chem Phys*. 1980;72(10):5639-5648. doi:10.1063/1.438980
88. Perdew JP, Wang Y. Accurate and simple analytic representation of the electron-gas correlation energy. *Phys Rev B*. 1992; 45(23):13244-13249. doi:10.1103/PhysRevB.45.13244
89. Staroverov VN, Scuseria GE, Tao J, Perdew JP. Comparative assessment of a new nonempirical density functional: molecules and hydrogen-bonded complexes. *J Chem Phys*. 2003; 119(23):12129-12137. doi:10.1063/1.1626543
90. Staroverov VN, Scuseria GE, Tao J, Perdew JP. Erratum: "Comparative assessment of a new nonempirical density functional: Molecules and hydrogen-bonded complexes" [J. Chem. Phys. 119, 12129 (2003)]. *J Chem Phys*. 2004;121(22):11507. doi:10.1063/1.1795692
91. Yanai T, Tew DP, Handy NC. A new hybrid exchange–correlation functional using the Coulomb-attenuating method (CAM-B3LYP). *Chem Phys Lett*. 2004;393(1–3):51-57. doi:10.1016/j.cplett.2004.06.011
92. Chai J-D, Head-Gordon M. Long-range corrected hybrid density functionals with damped atom-atom dispersion corrections. *Phys Chem Chem Phys*. 2008;10(44):6615-6620. doi:10.1039/b810189b
93. Chai J-D, Head-Gordon M. Systematic optimization of long-range corrected hybrid density functionals. *J Chem Phys*. 2008;128(8):084106. doi:10.1063/1.2834918
94. Schäfer A, Horn H, Ahlrichs R. Fully optimized contracted Gaussian basis sets for atoms Li to Kr. *J Chem Phys*. 1992; 97(4):2571-2577. doi:10.1063/1.463096
95. Schäfer A, Huber C, Ahlrichs R. Fully optimized contracted Gaussian basis sets of triple zeta valence quality for atoms Li to Kr. *J Chem Phys*. 1994;100(8):5829-5835. doi:10.1063/1.467146
96. Weigend F. Accurate Coulomb-fitting basis sets for H to Rn. *Phys Chem Chem Phys*. 2006;8(9):1057-1065. doi:10.1039/b515623h
97. Weigend F, Ahlrichs R. Balanced basis sets of split valence, triple zeta valence and quadruple zeta valence quality for H to Rn: design and assessment of accuracy. *Phys Chem Chem Phys*. 2005;7(18):3297-3305. doi:10.1039/b508541a
98. Zheng J, Xu X, Truhlar DG. Minimally augmented Karlsruhe basis sets. *Theor Chem Acc*. 2011;128(3):295-305. doi:10.1007/s00214-010-0846-z
99. Tao J, Perdew JP, Staroverov VN, Scuseria GE. Climbing the density functional ladder: nonempirical meta-generalized gradient approximation designed for molecules and solids. *Phys Rev Lett*. 2003;91(14):146401. doi:10.1103/PhysRevLett.91.146401
100. Dunning TH Jr. Gaussian basis sets for use in correlated molecular calculations. I. The atoms boron through neon and hydrogen. *J Chem Phys*. 1989;90(2):1007-1023. doi:10.1063/1.456153
101. Woon DE, Dunning TH Jr. Gaussian basis sets for use in correlated molecular calculations. III. The atoms aluminum through argon. *J Chem Phys*. 1993;98(2):1358-1371. doi:10.1063/1.464303
102. Becke AD. Density-functional thermochemistry. V. Systematic optimization of exchange-correlation functionals. *J Chem Phys*. 1997;107(20):8554-8560. doi:10.1063/1.475007
103. Grimme S. Semiempirical GGA-type density functional constructed with a long-range dispersion correction. *J Comput Chem*. 2006;27(15):1787-1799. doi:10.1002/jcc.20495
104. Grimme S, Ehrlich S, Goerigk L. Effect of the damping function in dispersion corrected density functional theory. *J Comput Chem*. 2011;32(7):1456-1465. doi:10.1002/jcc.21759

105. Schmider HL, Becke AD. Optimized density functionals from the extended G2 test set. *J Chem Phys*. 1998;108(23):9624-9631. doi:10.1063/1.476438
106. Kendall RA, Dunning TH Jr, Harrison RJ. Electron affinities of the first-row atoms revisited. Systematic basis sets and wave functions. *J Chem Phys*. 1992;96(9):6796-6806. doi:10.1063/1.462569
107. Polavarapu PL, Donahue EA, Hammer KC, et al. Chiroptical spectroscopy of natural products: avoiding the aggregation effects of chiral carboxylic acids. *J Nat Prod*. 2012;75(8):1441-1450. doi:10.1021/np300341z
108. Tsuneda T, Hirao K. Long-range correction for density functional theory. *WIREs Comput Mol Sci*. 2014;4(4):375-390. doi:10.1002/wcms.1178
109. Ravichandran L, Banik S. Performance of different density functionals for the calculation of vibrational frequencies with vibrational coupled cluster method in bosonic representation. *Theor Chem Acc*. 2017;137(1):1. doi:10.1007/s00214-017-2177-9
110. Barone V, Ceselin G, Fusè M, Tasinato N. Accuracy meets interpretability for computational spectroscopy by means of hybrid and double-hybrid functionals. *Front Chem*. 2020;8:8. doi:10.3389/fchem.2020.584203
111. Goerigk L, Grimme S. A thorough benchmark of density functional methods for general main group thermochemistry, kinetics, and noncovalent interactions. *Phys Chem Chem Phys*. 2011;13(14):6670-6688. doi:10.1039/c0cp02984j
112. Scholten K, Engelage E, Merten C. Basis set dependence of S═O stretching frequencies and its consequences for IR and VCD spectra predictions. *Phys Chem Chem Phys*. 2020;22(48):27979-27986. doi:10.1039/D0CP05420H
113. Vandenbussche J, Bultinck P, Przybył AK, Herrebout WA. Statistical validation of absolute configuration assignment in vibrational optical activity. *J Chem Theory Comput*. 2013;9(12):5504-5512. doi:10.1021/ct400843e
114. Covington CL, Polavarapu PL. Similarity in dissymmetry factor spectra: a quantitative measure of comparison between experimental and predicted vibrational circular dichroism. *J Phys Chem A*. 2013;117(16):3377-3386. doi:10.1021/jp401079s
115. Andernach L, Sandjo LP, Liermann JC, Buckel I, Thines E, Opatz T. Assignment of configuration in a series of dioxolanone-type secondary metabolites from *Guignardia bidwellii*—a comparison of VCD and ECD spectroscopy. *Eur J Org Chem*. 2013;2013(26):5946-5951. doi:10.1002/ejoc.201300530
116. Kauhl U, Andernach L, Weck S, et al. Total synthesis of (−)-hymenosetin. *J Org Chem*. 2016;81(1):215-228. doi:10.1021/acs.joc.5b02526
117. Andernach L, Opatz T. Assignment of the absolute configuration and total synthesis of (+)-caripyrin. *Eur J Org Chem*. 2014;2014(22):4780-4784. doi:10.1002/ejoc.201402540
118. Wink C, Andernach L, Opatz T, Waldvogel SR. Total synthesis of (±)-oxalicumone C and chiral resolution and elucidation of its absolute configuration. *Eur J Org Chem*. 2014;2014(35):7788-7792. doi:10.1002/ejoc.201403189
119. Casas ME, Kretschmann AC, Andernach L, Opatz T, Bester K. Separation, isolation and stereochemical assignment of imazalil enantiomers and their quantitation in an in vitro toxicity test. *J Chromatogr A*. 2016;1452:116-120. doi:10.1016/j.chroma.2016.05.008
120. Weber C, Pusch S, Schollmeyer D, Münster-Müller S, Pütz M, Opatz T. Characterization of the synthetic cannabinoid MDMB-CHMCZCA. *Beilstein J Org Chem*. 2016;12:2808-2815. doi:10.3762/bjoc.12.279
121. Pušavec Kirar E, Grošelj U, Golobič A, et al. Absolute configuration determination of 2,3-dihydro-1*H*,5*H*-pyrazolo[1,2-*a*]pyrazoles using chiroptical methods at different wavelengths. *J Org Chem*. 2016;81(23):11802-11812. doi:10.1021/acs.joc.6b02270
122. Dietz J-P, Lucas T, Groß J, et al. Six-step gram-scale synthesis of the human immunodeficiency virus integrase inhibitor dolutegravir sodium. *Org Process Res Dev*. 2021;25(8):1898-1910. doi:10.1021/acs.oprd.1c00139
123. Mirion M, Andernach L, Stobe C, et al. Synthesis and isolation of enantiomerically enriched cyclopenta[*b*]benzofurans based on products from anodic oxidation of 2,4-dimethylphenol. *Eur J Org Chem*. 2015;2015(22):4876-4882. doi:10.1002/ejoc.201500600

SUPPORTING INFORMATION

Additional supporting information can be found online in the Supporting Information section at the end of this article.

How to cite this article: Groß J, Kühlborn J, Pusch S, et al. Comparison of different density functional theory methods for the calculation of vibrational circular dichroism spectra. *Chirality*. 2023;35(10):753-765. doi:10.1002/chir.23580